Encapsulation of a double-helical water–nitrate chain inside unique double helical chiral channels formed from Keggin POM and hexaquo-cobalt(II) units

Rajarshi Chatterjee [a], Luna Paul [a], Dipak K. Hazra [b], Nabanita Pal [a], Atish Dipankar Jana [c], Monika Mukherjee [b], Mahammad Ali [a,*]

[a] *Department of Chemistry, Jadavpur University, Kolkata 700 032, India*
[b] *Department of Solid State Physics, Indian Association for the Cultivation of Science, Jadavpur, Kolkata 700 032, India*
[c] *Department of Physics, Behala College, Kolkata 700 060, India*

ABSTRACT

A new inorganic–organic hybrid chiral molecule $[Co(H_2O)_6][C_5H_6N]H_4[CoW_{12}O_{40}]NO_3 \cdot 3H_2O$ has been prepared by the hydrothermal method and was characterized by elemental analysis, IR and UV spectra, TG-DTA and single crystal X-ray diffraction techniques. The asymmetric unit consists of $[CoW_{12}O_{40}]^{6-}$ and NO_3^- anions, the charge of which are counterbalanced by one octahedral $[Co(H_2O)_6]^{2+}$ cation, a pyridinium $[C_5H_6N]^+$ ion and $4H^+$ ions. The molecular structure of the title complex reveals a 3D supramolecular framework formed through intermolecular hydrogen bonds. This constitutes the first example in which a chiral architecture has been generated from achiral building blocks, where centro-symmetrically related cobalt octahedra and polyoxoanion tetrahedra are entangled through pairs of hydrogen bonds in a double helical way with a channel that houses a 1D water–NO_3^- double helix. This chiral POM shows good efficiency in the oxidation of common olefins in the presence of an environmentally benign oxidant, H_2O_2, under mild conditions.

© 2013 Elsevier Ltd. All rights reserved.

1. Introduction

The design and synthesis of chiral polyoxometallates (POMs) have become a topic of immense interest owing to their intriguing variety of architectures and topologies. Their uniqueness is also manifested by their potential applications in medicine and asymmetric catalysis [1]. As chirality is a crucial issue in fields ranging from chemistry to material as well as biological sciences, the preparation of chiral POMs is consequently a goal for many polyoxometallate chemists, as it would provide ultimate control of the synthesis of these nano-sized objects. However, only a handful of chiral compounds containing polyoxoanions have been reported so far [2]. In general, two different synthetic strategies have been adopted to build chiral POM based architectures. These are: (i) stitching of chiral organic linkers or chiral metal complexes with achiral POMs clusters, transferring the chirality from the chiral source to the final architectures; [3–5] (ii) use of achiral ligands for breaking of the symmetry with spontaneous resolution without any chiral auxiliaries which yields a conglomerate, i.e. a racemic mixture of chiral crystals [6]. However, the second approach, lead-

ing to the formation of chiral POM based 3D architectures, faces some fundamental questions, like: (a) how is a chiral block generated from achiral components without a chiral auxillary? (b) how can the highly symmetric POM loses its symmetry and allow the structure to get crystallized in a non-centrosymmetric space group? Therefore, the search for suitable achiral organic molecules, metal cations and POM building units to be applied in the construction of chiral 3D frameworks is one of the most challenging issues in synthetic chemistry and materials science. Among the many different types of POMs, the most well known are the Keggin heteropolyanions. Although it has been amply demonstrated that these clusters can be linked into low-dimensional (0D, 1D or 2D) structures using metal cations or their coordination complexes as linkers, [7] the process of assembling Keggin POMs into 3D frameworks is still in its infancy; perhaps owing to its steric demands and the deficient charge density at its surface oxygen atoms. Recently, a chiral framework composed of achiral building units in enantiomorphic crystals was reported, but here the covalent assembly of achiral metal-complex linkers and achiral POM building blocks were involved [8]. To our understanding there might be another approach where chirality may also be imposed into the architecture generated through non-bonding interactions among different achiral entities, like transition metal complexes, organic

ligands and the POM unit. To the best of our knowledge, there is no such single report on this approach. Not only that, to date only a restricted number of chiral assemblies of Keggin POM based compounds have been observed, and most of them are discrete or low-dimensional structures [9,10]. In the case of the trilacunary Keggin $[\alpha\text{-}PMo_9O_{31}(OH_2)_3]^{3-}$, the longer bond length to the aqua ligand shortens the trans Mo–O bond, which in turn lengthens the next O–Mo bond, and so on, resulting in two enantiomers [9]. Miwa and co-workers [10] demonstrated that Keggin-type heteropolyanions of the general formula $[XM_{12}O_{40}]^{n-}$ (with X = Co^{II}, Zn^{II}, 2H$^+$ and Al^{III}) presented induced Cotton effects in the presence of L-brucinium cations, and optical resolutions were carried out using a chiral protonated amino acid, but no structures were reported. Here, we have attempted to explore a hydrothermal route for the preparation of such a chiral hybrid material based on a Keggin heteropolyanion using simple reactants and have reported the structure and properties of a new chiral inorganic–organic hybrid Keggin complex, $[Co(H_2O)_6][C_5H_6N]H_4[CoW_{12}O_{40}][NO_3]\cdot 3H_2O$, that generates a 3D motif through H-bonding interactions. The most striking features are the generation of a chiral channel through the entangling of $[Co(H_2O)_6]^{2+}$ and $[CoW_{12}O_{40}]^{6-}$ units, which suitably houses a double helical chain constructed from water molecules and NO_3^- anions. Effective conversions of various olefins via liquid phase oxidation reactions are also observed over this chiral molecule due to the presence of its oxidizing metal environment [11].

2. Experimental

2.1. Materials

Chemicals like Na_2WO_4 (AR Loba, India), $Co(NO_3)_2\cdot 6H_2O$ (AR Loba, India), pyridine (Merck, India) etc. were of reagent grade and were used as received. Deionized water was used as the solvent.

2.2. Physical measurements

Elemental analyses were carried out using a Perkin–Elmer 240 elemental analyzer. The FTIR spectra were recorded as Nujol mulls at ambient temperatures between the ranges 400–4000 cm^{-1}. The spectra were recorded on a Nicolet Magna IR 750 series-II FTIR spectrophotometer using KBr pellets. TG analyses were performed on a Perkin–Elmer Pyris Diamond TGA/DTA Analyzer in flowing N$_2$ with a heating rate of 10 °C min^{-1}.

2.3. Catalytic reactions

Liquid phase oxidation reactions of styrene and cyclohexene were carried out using this material as the catalyst and hydrogen peroxide (H$_2$O$_2$) as the oxidant. The overall reaction was performed in a two necked round-bottomed flask fitted with a condenser and using a temperature-controlled oil bath on a magnetic stirrer. In a typical procedure, 0.5 g of the substrate was taken with the same molar ratio of H$_2$O$_2$ (30%, Merck, India) in 5.0 ml acetonitrile solvent, containing the required amount of the catalyst. The temperature of the reaction was maintained at 60 °C and the products were collected at regular intervals. The progress of the reaction was monitored with an Agilent 7890D gas chromatograph (FID detector) fitted with a capillary column. The products were identified by comparing with known standards. The products of cyclohexene oxidation were confirmed by GCMS-Shimadzu-QP5050A GCMS-E1 analysis.
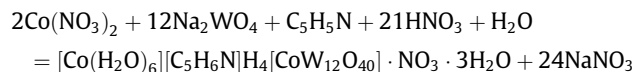
2.4. X-ray crystallography

X-ray diffraction data for **1** were collected at 298(2) K on a Bruker SMART APEX CCD X-ray diffractometer using graphite-monochromated Mo Kα radiation (λ = 0.71073 Å). Determination of integrated intensities and cell refinement were performed with the SAINT [12] software package using a narrow-frame integration algorithm. An empirical absorption correction [13] (SADABS) was applied. The structure was solved by direct-methods with SHELXS-97 and refined using full-matrix least-squares techniques against F^2 with anisotropic displacement parameters for non-hydrogen atoms with SHELXL-97 [14], except for water molecules of crystallization. Hydrogen atoms (except those for water of crystallization) were placed at calculated positions using suitable riding models with isotropic displacement parameters derived from their carrier atoms. In the final difference Fourier maps there were no remarkable peaks except the ghost peaks surrounding the tungsten atom and near disordered water molecules. A summary of the crystal data and relevant refinement parameters for **1** are provided in Table 1.

2.5. Synthesis of the complex $[Co(H_2O)_6][C_5H_6N]$ $H_4[CoW_{12}O_{40}][NO_3]\cdot 3H_2O$ (**1**)

The title compound was prepared by the hydrothermal method from a vigorously stirred, as well as heated, acidic mixture (acidified by adding 10 ml of 6(N) HNO$_3$) of 2.97 g (9 mmol) Na$_2$WO$_4\cdot$2H$_2$O and 0.58 g (2 mmol) Co(NO$_3$)$_2\cdot$6H$_2$O in 25 ml of water. The resulting pH was adjusted to 5.0 by the dropwise addition of 5 ml of pyridine. The entire mixture was then transferred into a Teflon jacket in a PTTE-lined stainless steel pressure vessel and was kept in an oven at 160 °C for five consecutive days under autogeneous pressure. The solution was cooled by decreasing the temperature at regular intervals of 5 °C over one day. After cooling the autoclave to room temperature, green block-shaped crystals were obtained, filtered, washed several times with distilled water and dried in air (yield 25% based on W). The composition of the complex was determined by elemental *Anal.* Calc. based on C$_5$H$_{28}$Co$_2$N$_2$O$_{52}$W$_{12}$: C, 1.83; H, 0.86; N, 0.86. Found: C, 1.85; H, 0.88; N, 0.87%. The following chemical reaction is expected:

Table 1
Crystal data and structure refinement parameters for **1**.

Formula	C$_5$H$_{24}$Co$_2$N$_2$O$_{52}$W$_{12}$
Formula weight	3268.32
Crystal system	hexagonal
Space group	P6222 (No.180)
a (Å)	12.0914(14)
b (Å)	12.0914(14)
c (Å)	33.296(8)
V (Å^3)	4215.8(12)
Z	6
D_{calc} (g/cm^3)	4.049
M(Mo Kα) (mm)	50.243
$F(000)$	4514
Crystal size (mm)	0.02 × 0.21 × 0.32
T (K)	298
Radiation (Å) Mo Kα	0.71073
θ Min–Max (°)	1.8–20.6
Dataset	−11: 11; −11: 11; −31: 32
Tot., Uniq. Data, R_{int}	26077, 1428, 0.104
Observed data [$I > 2.0\sigma(I)$]	1347
Nref, Npar	1428, 208
R, wR_2, S	0.0518, 0.1344, 1.21
Max. and Av. Shift/Error	0.01, 0.00
Flack	0.97(7)
Min. and Max. Resd. Dens. (e/Å^3)	−1.24, 1.74

$$2Co(NO_3)_2 + 12Na_2WO_4 + C_5H_5N + 21HNO_3 + H_2O$$

$$= [Co(H_2O)_6][C_5H_6N]H_4[CoW_{12}O_{40}] \cdot NO_3 \cdot 3H_2O + 24NaNO_3$$

2.6. Structural description

The crystal structure is composed of a Keggin-type $[CoW_{12}O_{40}]^{6-}$ anion, one hexa aqua cobalt $[Co(H_2O)_6]^{2+}$ counter cation and three water molecules of crystallization, along with one NO_3^- group and one pyridinium $[C_5H_6N]^+$ ion. The oxygen atom (O14) of the solvent water molecules in **1**, located near (1, 0, 1/6) was disordered between two centrosymmetrically related positions. The dodecatungstocobaltate $[CoW_{12}O_{40}]^{6-}$ consists of four vertex-sharing trinuclear W_3O_{13} triad units, each of which is made up of three edge-sharing WO_6 octahedra around the CoO_4 central tetrahedron (Fig. 1) [15,16]. According to the different coordination fashions of the oxygen atoms in the Keggin unit, the O atoms can be classified into three groups, i.e. unshared or terminal O atoms 'O_t', bridging O atoms (O_b) connecting two W atoms, and O atoms (O_c) of the central CoO_4 unit. The $W–O_t$ bond lengths vary between 1.66(2) and 1.73(2) Å, while the $W–O_b$ and $W–O_c$ bond distances lie in the range 1.88(2)–1.97(2) and 2.13(2)–2.20(2) Å, respectively. In the CoO_4 tetrahedron, the metal center (Co1) is seated at the intersection of three two-fold rotation axes with coordinates (½, 0, 0). The coordination geometry around the Co atom is distorted tetrahedral, which is reflected by the central Co–O bond lengths [1.88(2) Å] and the O–Co–O angles [108.1(14)–111.8(14)°]. From the variation of the W–O distances and the bond angles around the W atoms, it is evident that there is considerable distortion in the WO_6 octahedra in the complex. This is consistent with the structural features of polyoxotungstates exhibiting Keggin structures [16–18]. Another part of compound **1** is the presence of a discrete cobalt complex, where the metal atom is surrounded by six molecules of water forming the cation. The Co (Co2) atom is in a nearly regular octahedral coordination geometry, with Co–O distances between 1.99(4) and 2.07(4) Å, and angles ranging from 87.4(12)° to 92.6(12)°, which are comparable with the reported values for related hexa aqua
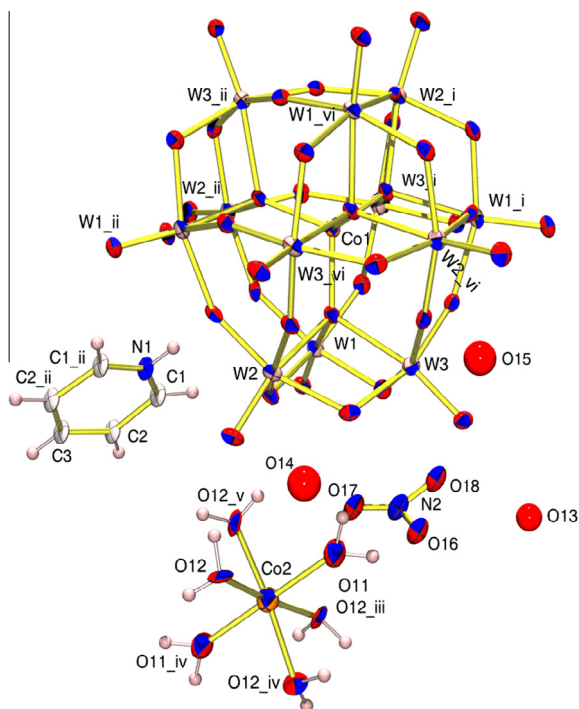
cobalt complexes [19–21]. Four oxygen atoms lying on the mirror plane, O12 and those generated by the symmetry operations $(-x + 2, -x + y + 1, -z + 1/3, x, x - y, -z + 1/3, -x + 2, -y + 1, z)$, define the basal plane and the remaining two oxygen atoms, O11 and the symmetry $(-x + 2, -x + y + 1, -z + 1/3)$ related oxygen atom, lying on the four-fold axis occupy the axial sites. Selected bond distances and angles are given in Table 2. The hexa aquo cobalt(II) units play a decisive role in the 3D supramolecular organization of the complex. Each hexa aquo cobalt(II) unit acts as a nodal point of a tetrahedral network (Fig. S1) through strong O–H⋯O (Table 3) hydrogen bonds connecting four adjacent POM units in a tetrahedral geometry. A part of this network propagating along the [0 0 1] direction is shown in Fig. 2. Here centrosymmetrically related cobalt octahedra and polyoxoanion tetrahedra are connected through pairs of O12–H12A⋯O4 $(1-x, 1 - x + y, 1/3 - z)$ hydrogen bonds, which according to the graph-set notation can be described as an $R_6^6(36)$ ring (Fig. 3). Intermolecular O11–H11⋯O6 $(1 - x, 1 - y, z)$ and O12–H12⋯O3 $(1-x, 1 - y, z)$ hydrogen bonds link the $[Co(H_2O)_6]^{2+}$ cation and the polyoxoanion. Along the [0 0 1] direction, the $[Co(H_2O)_6]^{2+}$ units and the POM units are wound in a double helical way (Fig. 4a), generating a channel along the crystallographic c-axis (Fig. 4b) which encapsulates a unique 1D $H_2O–NO_3^-$ double helical assembly (Fig. 4c). Adjacent $[Co(H_2O)_6]^{2+}$–$H_4[CoW_{12}O_{40}]^{2-}$ double helices are fused with each other and a 3D supramolecular chiral tetrahedral network is formed. It should be pointed out that due to the relatively larger size of the POM units than the hexa aquo cobalt(II) units, even after fusion of successive helices there remains an inter-groove vacant space which accomodates pyridinium ions. The pyridinium ion acts as a suitable H-donor for the Keggin terminal O acceptors, simultaneously donating to four O atoms of the same Keggin POM unit that vertically land on the centre of the cap of the Keggin unit (Fig. 5). The pyridinium ion also establishes a bifurcated CH⋯O bond with two other Keggin units on the other sides, leading to 2D layers (Fig. 6) and interact with $[Co(H_2O)_6]^{2+}$ units in a plane with the Keggin units lying above and below this plane (Fig. S2). Double helical compounds generally consist of the same coordination, supramolecular or covalent chains [22], and here we observed the unique double helix constructed through supramolecular assemblies (Fig. S3). It is noted that the achiral ligand and metal ion may not produce a helical structure that is exclusively right-handed or left-handed, which always results in a racemic mixture of right- and left-handed helical products. In the present structure, the hexa-aquo cobalt cation is responsible for induction of chirality in the assembly, resulting a racemic mixture. The coordinated water molecules to Co in the $[Co(H_2O)_6]^{2+}$ ion act as hydrogen bond donors for the Keggin POM units. In the octahedral coordination geometry of Co, two adjacent water molecules, one attached axially

Fig. 1. ORTEP view (30% ellipsoidal probability) of the title compound 1.

Table 2
Selected bond lengths (Å) and angles (°) with esd's in parentheses for **1**.

|			
W(1)–O(10)	1.66(2)	W(2)–O(1)	2.13(2)
W(1)–O(2)	1.92(2)	W(3)–O(9)	1.68(2)
W(1)–O(4)	1.92(3)	W(3)–O(7)	1.89(2)
W(1)–O(7)#1	1.95(2)	W(3)–O(5)	1.90(2)
W(1)–O(8)	1.95(2)	W(3)–O(6)	1.91(2)
W(1)–O(1)	2.20(2)	W(3)–O(2)	1.97(2)
W(2)–O(3)	1.73(2)	W(3)–O(1)	2.17(2)
W(2)–O(8)#2	1.88(2)	Co(1)–O(1)	1.88(2)
W(2)–O(4)	1.91(2)	Co(2)–O(11)	1.99(4)
W(2)–O(5)#3	1.92(2)	Co(2)–O(12)	2.07(4)
W(2)–O(6)	1.95(3)		
O(1)#1–Co(1)–O(1)#2	108.1(14)	O(11)#4–Co(2)–O(12)#4	87.4(12)
O(1)–Co(1)–O(1)#1	111.8(14)	O(11)–Co(2)–O(12)#4	92.6(12)

Symmetry codes: #1 $x - y, -y, -z$ #2 $-x + 1, -y, z$ #3 $-x + y + 1, y, -z$ #4 $-x + 2, -x + y + 1, -z + 1/3$.

Table 3
Intermolecular contacts of the compound (Å, °).

D–H···A	(D–H)	d(H···A)	d(D···A)	D–H···A
N(1)–H(1)···O(4)i	0.85	2.56	3.11(8)	123
N(1)–H(1)···O(8)i	0.85	2.45	3.15(9)	141
O(11)–H(11)···O(6)ii	0.87	2.26	3.08(4)	157
O(12)–H(12)···O(3)ii	0.88	2.14	2.97(5)	158
O(12)–H(12A)···O(4)iii	0.81	2.27	2.97(6)	145
C(3)–H(3)···O(9)iv	0.93	2.28	3.00(5)	134

Symmetry codes: (i) x, $x − y$, $1/3 − z$ (ii) $1 − x$, $1 − y$, z (iii) $1 − x$, $1 − x + y$, $1/3 − z$ (iv) $x − y$, $1 − y$, $−z$.

and the other equatorially, simultaneously donate water protons to a particular Keggin unit. This simultaneous H-bonding of equatorial and axial water molecules to four adjacent Keggin units by a particular hexa aquo cobalt unit is responsible for the appearance of helicity and chirality in the assembly. Moreover, as the cluster as a whole is neutral, it follows from the charge balance that the cobalt atom of both the hexaaqua cobalt ion and the cobalt atom of the CoO_4 tetrahedron in the Keggin polyoxoanion must prevail in the +2 oxidation state. In order to confirm these valence-state attributions, bond valence sum (BVS) calculations [23–25] were performed for each cobalt, tungsten and oxygen centre. On the basis of charge balance, the oxidation state of the central atom could be confidently ascertained from bond valence sum (BVS) calculations. The working formula is BVS = $\Sigma \exp[(r_0 − r)/B]$ where r is the observed bond distance and r_0 and B are empirically determined parameters;
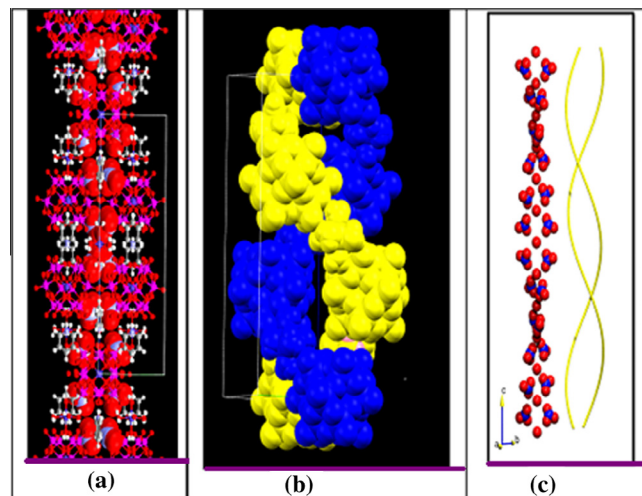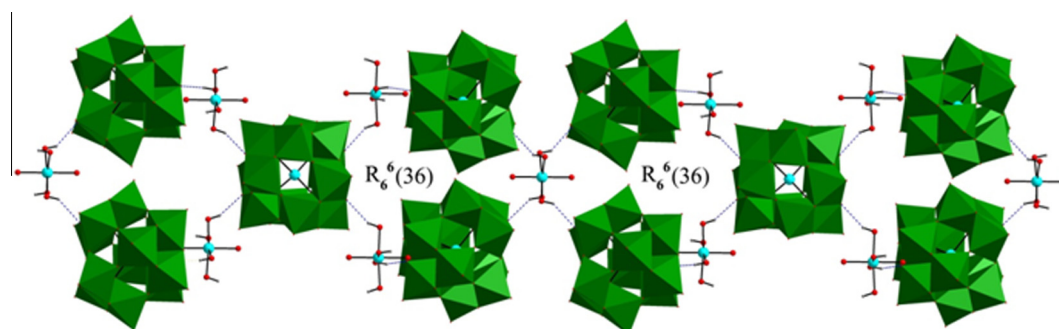

Fig. 4. (a) The supramolecular assembly of $[Co(H_2O)_6]^{2+}$ and $H_4[CoW_{12}O_{40}]^{2−}$ units giving rise to channels arranged in a hexagonal symmetry; (b) The channel formed by double helically wound Keggin POM units (blue) and $[Co(H_2O)_6]^{2+}$ units (yellow) with a channel inside; (c) The $H_2O–NO_3^{−}$ double helix that resides inside the channel. (Colour online.)

$r_0 = 1.921$ Å for $W^{6+}–O^{2−}$, $r_0 = 1.692$ Å for $Co^{2+}–O^{2−}$ and $B = 0.37$, which is a constant. The BVS values of tungsten atoms in the polyoxo moiety, listed in SUP Tables 4a–c, i.e. for W(1), W(2) and W(3),
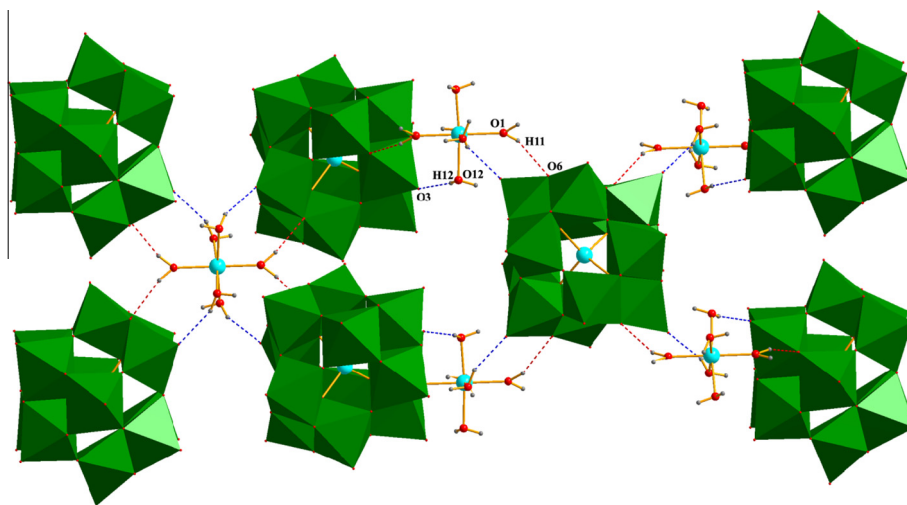
Fig. 2. Intermolecular O11–H11···O6 (red) and O12–H12···O3 (blue) hydrogen bonds link the hexa aqua cobalt cation and polyoxoanion to form a one-dimensional infinite chain propagating along the [0 0 1] direction. (Colour online.)

Fig. 3. Pairs of O12–H12A O4 hydrogen bonds forming an R_6^6 (36) ring.
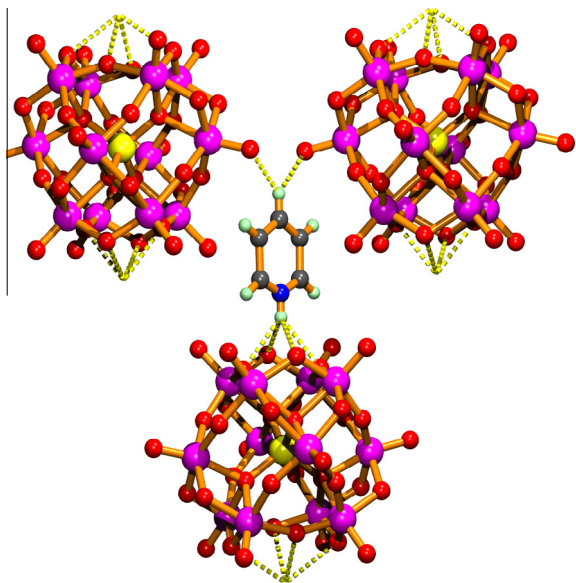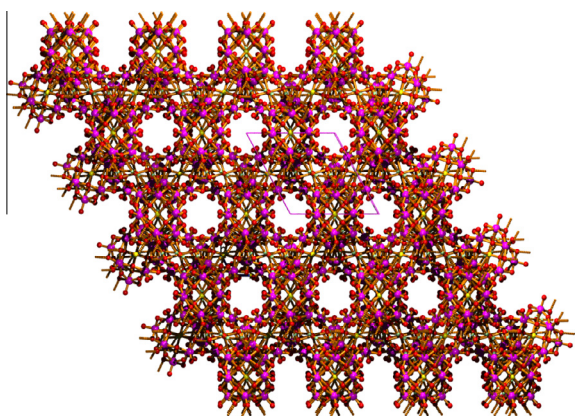
Fig. 5. The hydrogen bonded pyridinium ion.

Fig. 6. The supramolecular assembly of POMs and pyridinium ions.

Table 4
Variation of solvents for the oxidation of styrene.

Solvent	Product conversion (%)
Water	No conversion
Acetonitrile	49.1
Dichloromethane	2.0
Toluene	0.4

are 6.36, 6.32 and 6.48 respectively, which gives an average value of 6.38 for the calculated oxidation state of W. The BVS values of cobalt (2.40) and tungsten (6.38) in the polyoxoanion $[CoW_{12}O_{40}]^{6-}$ and cobalt (2.33) in $[Co(H_2O)_6]^{2+}$, listed in Tables S1–S3, beautifully agreed with a +2 valence state of cobalt and +6 valence state of tungsten in $[CoW_{12}O_{40}]^{6-}$ and +2 valence state of cobalt in $[Co(H_2O)_6]^{2+}$. In short, all the atoms fall within the expected bond valence limits. Besides this, charge balance considerations also dictate that in addition to the two protons associated with the tungsten core, there must be an additional protonation site at the periphery of the polyoxo cluster accomodating two additional protons. Valence sum calculations on the four triply bridging oxo-groups (W_3O) which lie in the cavity of the cluster provide oxygen valences of 1.5, clearly consistent with two protons delocalized over these sites. Correspondingly, the crystallographic data does not allow a definite assignment of the protonation site.

2.7. IR analysis

The IR spectrum of the title compound has some characteristic bands for the polyoxoanion at 941, 878, 770 and 448 cm^{-1}, which are attributed to v(W=O$_t$ terminal), v(W–O$_b$–W octahedral edge sharing), v(W–O$_c$–W octahedral corner sharing) and v(Co–O tetrahedral), respectively, whereas for the pyridinium cation, bands have been observed at 685, 7465, 1255, 1385, 1483, 1546, 1691 and 3170 cm^{-1}. Features at 1255, 1483 and 1691 cm^{-1} are attributed to stretching vibrations of (C–H), (C–C) and (C=N) bonds respectively. The v(N–H) vibrations appear at 3170 cm^{-1} in the IR spectrum of pyH$^+$. The v(Co–O) band of the discrete octahedral hexa aquo Co(II) cation is assigned at 502 cm^{-1}. In addition, a strong broad peak observed at 3570 cm^{-1} is assigned to a v(−OH) absorption along with hydrogen bonds, which proves the
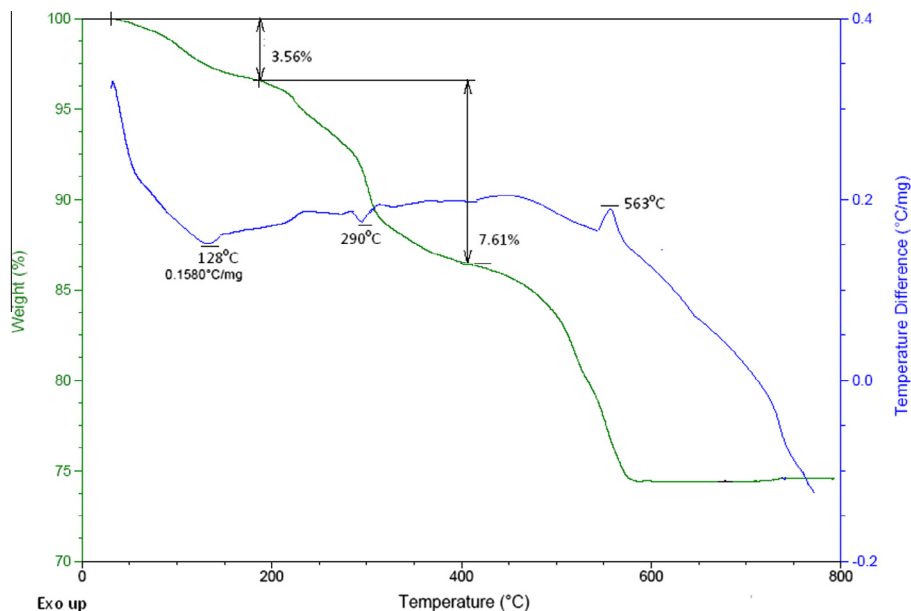

Fig. 7. TGA of the complex $[Co(H_2O)_6][C_5H_6N]H_4[CoW_{12}O_{40}][NO_3]\cdot3H_2O$ in the range 40–575 °C.

Table 5
Oxidation of olefines over this chiral POM.

Substrate	Conversion (%)	Main product	Selectivity (%)
Styrene	49.10	Benzaldehyde	85.44
Cyclohexene	97.04	Cyclohexene-1-one	79.65

Reaction conditions: 0.50 g substrate, 0.55 g 30% H_2O_2, 5 ml acetonitrile, 0.02 g catalyst, 60 °C temperature, maximum time 24 h.

presence of lattice water. Comparing with the IR spectrum of $[CoW_{12}O_{40}]^{6-}$, the vibrational frequencies of the W–O bonds have shifted to lower wavenumbers, showing the interaction of the polyoxoanions and cations as well as lattice water (Fig. S4) [26].

2.8. Thermogravimetric analysis

The thermal decomposition profile (Fig. 7) of the title compound gives a total weight loss of 11.17% (calculated 11.53%) in the range 40–575 °C. The mass loss in the two initial phases may arise from the reaction: $[Co(H_2O)_6]^{2+} + NO_3^- + PyH^+ + 3H_2O + 5OH^- 4H^+ \rightarrow CoO + NO_2 + Py + 14 H_2O$, and the corresponding weight loss is 11.53%. The first phase of weight loss in the TGA curve may correspond to the overall loss of 6 water molecules (3 lattice water molecules plus two from $Co(H_2O)_6^{2+}$ [27] and 1 from surface protonated OH groups of the POM moiety, leading to a weight loss of 3.30% (experimental 3.56%). In the second stage, the weight loss of 8.23% (experimental 7.61%) in the range 175–410 °C corresponds to the overall decomposition of the $[Co(H_2O)_4]^{2+}$ ion, leading to the loss of $4H_2O$ and rest of the surface OH- groups ($2H_2O$), one pyridine molecule and one NO_3^- anion, giving a weight loss of 8.23%. These are followed by two endothermic peaks at 128 and 290 °C respectively in the DTA curve. After that the compound undergoes thermal decomposition.

2.9. Catalysis

We investigated the catalytic activity of this chiral polyoxometallate for the oxidation of styrene and cyclohexene in the presence of hydrogen peroxide. Acetonitrile under homogeneous conditions has been proven to be an appropriate solvent for this reaction, because other polar and non-polar solvents fail to produce any significant yield. The data is shown in Table 4. The results of oxidation are presented in Table 5. In the case of styrene, although the total conversion is quite low after 6 h reaction (only 48.05%), the selectivity towards benzaldehyde is quite high (87.80%), and after a
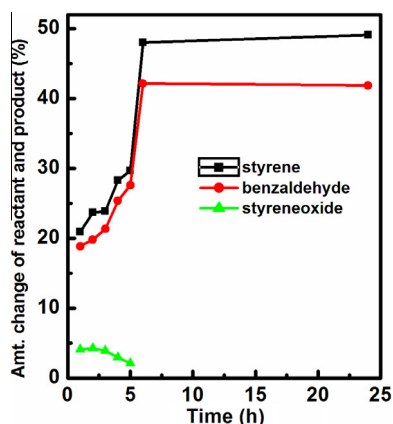
Fig. 8. Styrene conversion and benzaldehyde/styrene oxide formation with respect to time.
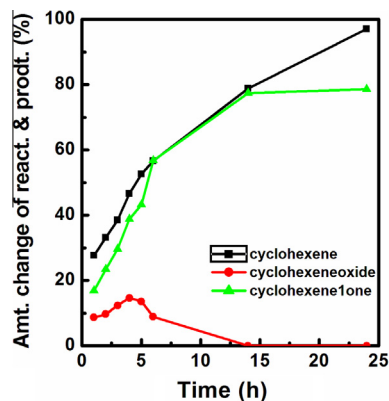
Fig. 9. Cyclohexene conversion and cyclohexene oxide formation with respect to time.

prolonged reaction time of 24 h, only a small amount of benzoic acid is produced (7.16%). The styrene conversion and formation of products after different time intervals are graphically shown in Fig. 8. The conversion of styrene oxide was very low and a maximum was reached after 2 h (ca. 6%). The total conversion of cyclohexene after 24 h was very high with cyclohexene-1-one as the main product, though cyclohexene oxide was found with a maximum yield after 6 h of 13.6% (confirmed by GCMS). Afterwards this oxide was readily converted to cyclohexene-1-ol and then cyclohexene-1-one, owing to further oxidation which is evident from the disappearance of the cyclohexene oxide peak after 6 h. There is another product, cyclohexene-1-ol, which is obtained in about 15% after 24 h. A graphical plot, given in Fig. 9, shows the change of reactant and product amounts with time. There is no observable conversion of the products at room temperature.

3. Conclusions

A novel inorganic–organic hybrid compound composed of Keggin tungstocobaltate has been synthesized by a hydrothermal method in a one-pot reaction by the interaction of the composing elements without the need for any polyoxoanion precursor species, and its crystal structure was solved by single crystal X-ray diffraction techniques. The molecular structure of the title complex reveals the formation of a three-dimensional supramolecular framework by a combination of intermolecular hydrogen bonds. Here, we disclose for the first time the generation of a chiral architecture from achiral building blocks comprising of a metal ion, a carbon ammonium ion and a Keggin POM through non-covalent (H-bonding) interactions. The $[Co(H_2O)_6]^{2+}$ unit plays a crucial role in the 3D supramolecular organization, acting as a nodal point of a tetrahedral network through strong O–H···O hydrogen bonds, connected to four adjacent POM units in a tetrahedral geometry. The centrosymmetrically related cobalt octahedra and polyoxoanions tetrahedra are entangled through pairs of hydrogen bonds in a double helical way with a channel that houses a 1D water-NO_3^- double helix. This chiral POM shows good efficiency in the oxidation of common olefins in the presence of the environmentally benign oxidant H_2O_2 under mild conditions.

Appendix A. Supplementary data

CCDC 865046 contains the supplementary crystallographic data for **1**. These data can be obtained free of charge via http://www.ccdc.cam.ac.uk/conts/retrieving.html, or from the Cambridge Crystallographic Data Centre, 12 Union Road, Cambridge CB2 1EZ, UK; fax: (+44) 1223-336-033; or e-mail: deposit@ccdc.cam.ac.uk. Supplementary data associated with this article can be found, in the online version, at http://dx.doi.org/10.1016/j.poly.2013.10.027.

References

[1] (a) A. Müller, F. Peters, M.T. Pope, D. Gatteschi, Chem. Rev. 98 (1998) 239;
(b) D.A.J. Judd, H. Nettles, N. Nevins, J.P. Snyder, D.C. Liotta, J. Tang, J. Ermolieff, R.F. Schinazi, C.L. Hill, J. Am. Chem. Soc. 123 (2001) 886.
[2] (a) T.A. Sullens, R.A. Jensen, T.Y. Shvareva, T.E. Albrecht-Schmitt, J. Am. Chem. Soc. 126 (2004) 2676;
(b) H.-Y. An, E.-B. Wang, D.-R. Xiao, Y.-G. Li, Z.-M. Su, L. Xu, Angew. Chem., Int. Ed. 45 (2006) 904;
(c) L. Cai, Y. Li, C. Yu, H. Ji, Y. Liu, S. Liu, Inorg. Chim. Acta 362 (2009) 2895;
(d) H. Tan, Y. Li, Z. Zhang, C. Qin, X. Wang, E. Wang, Z. Su, J. Am. Chem. Soc. 129 (2007) 10066;
(e) Y. Zhang, L. Zhang, Z. Hao, F. Luo, Dalton Trans. 39 (2010) 7012;
(f) C. Qin, X.-L. Wang, L. Yuan, En-Bo Wang, Crystal Growth Des. 8 (2008) 2093;
(h) X. Fang, T.M. Anderson, Y. Hou, C.L. Hill, Chem. Commun. (2005) 5044;
(i) Y. Hou, X. Fang, C.L. Hill, Chem. Eur. J. 13 (2007) 9442;
(j) J. Zhang, J. Hao, Y. Wei, F. Xiao, P. Yin, L. Wang, J. Am. Chem. Soc. 132 (2010) 14;
(k) H. Naruke, J. Iijima, T. Sanji, Inorg. Chem. 50 (2011) 7535.
[3] (a) A. von Zelewsky, U. Knof, Angew. Chem., Int. Ed. 38 (1999) 302;
(b) C.J. Kepert, T.J. Prior, M.J. Rosseinsky, J. Am. Chem. Soc. 122 (2000) 5158;
(c) T.J. Prior, M.J. Rosseinsky, Inorg. Chem. 42 (2003) 1564;
(d) T. Ezuhara, K. Endo, Y. Aoyama, J. Am. Chem. Soc. 121 (1999) 3279;
(e) Y. Cui, H.L. Ngo, W.B. Lin, Chem. Commun. (2003) 1388;
(f) R.-G. Xiong, X.-Z. You, B.F. Abrahams, Z.-L. Xue, C.-M. Che, Angew. Chem., Int. Ed. 40 (2001) 4422.
[4] (a) F.B. Xin, M.T. Pope, J. Am. Chem. Soc. 118 (1996) 7731;
(b) M. Inoue, T. Yamase, Bull. Chem. Soc. Jpn. 68 (1995) 3055;
(c) M. Inoue, T. Yamase, Bull. Chem. Soc. Jpn. 69 (1996) 2863;
(d) D.L. Long, P. Kogerler, L.J. Farrugia, L. Cronin, Chem. Asian J. 1 (2006) 352;
(e) D.L. Long, E. Burkholder, L. Cronin, Chem. Soc. Rev. 36 (2007) 105;
(f) C. Streb, D.L. Long, L. Cronin, Chem. Commun. (2007) 471;
(g) U. Kortz, M.G. Savelieff, F.Y.A. Ghali, L.M. Khalil, S.A. Maalouf, D.I. Sinno, Angew. Chem., Int. Ed. 41 (2002) 4070;
(h) X.K. Fang, T.M. Anderson, C.L. Hill, Angew. Chem., Int. Ed. 44 (2005) 3540;
(i) X.K. Fang, T.M. Anderson, Y. Hou, C.L. Hill, Chem. Commun. (2005) 5044;
(j) L.M. Zheng, T. Whitfield, X. Wang, A.J. Jacobson, Angew. Chem., Int. Ed. 39 (2000) 4528.
[5] (a) H.Y. An, E.B. Wang, D.R. Xiao, Y.G. Li, Z.M. Su, L. Xu, Angew. Chem., Int. Ed. 45 (2006) 904;
(b) H.Q. Tan, Y.G. Li, Z.M. Zhang, C. Qin, X.L. Wang, E.B. Wang, Z.M. Su, J. Am. Chem. Soc. 129 (2007) 10066.
[6] (a) T. Matsuura, H. Koshima, J. Photochem. C Rev. 6 (2005) 7;
(b) D.K. Kondepudi, R. Kaufman, N. Singh, Science 250 (1990) 975;
(c) X.D. Chen, M. Du, T.C.W. Mak, Chem. Commun. (2005) 4417;
(d) M. Sasa, K. Tanaka, X.-H. Bu, M. Shiro, M. Shionoya, J. Am. Chem. Soc. 123 (2001) 10750;
(e) U. Siemeling, I. Scheppelmann, B. Neumann, A. Stammler, H.G. Stammler, J. Frelek, Chem. Commun. (2003) 2236;
(f) F.M. Tabellion, S.R. Seidel, A.M. Arif, P.J. Stang, Angew. Chem., Int. Ed. 40 (2001) 1529;
(g) Y.T. Wang, M.L. Tong, H.H. Fan, H.Z. Wang, X.M. Chen, Dalton Trans. (2005) 424;
(h) Q.Z. Sun, Y. Bai, G.J. He, C.Y. Duan, Z.H. Lin, Q.J. Meng, Chem. Commun. (2006) 2777;
(i) S. Jayanty, T.P. Radhakrishnan, Chem. Eur. J. 10 (2004) 2661.
[7] M. Nyman, F. Bonhomme, T.M. Alam, M.A. Rodriguez, B.R. Cherry, J.L. Krumhansl, T.M. Nenoff, A.M. Sattler, Science 297 (2002) 996.
[8] Y.-Q. Lan, S.-L. Li, Z.-M. Su, K.-Z. Shao, J.-F. Ma, X.-L. Wang, E.-B. Wang, Chem. Commun. (2008) 58.
[9] R. Strandberg, Acta Chem. Scand. A. A28 (1974) 217.
[10] K. Nomiya, R. Kobayashi, M. Miwa, T. Hori, Polyhedron 3 (1984) 1071.
[11] E. Poli, R. De Sousa, F. Jérome, Y. Pouilloux, J.-M. Clacens, Catal. Sci. Technol. 2 (2012) 910.
[12] Bruker, APEX2, SAINT XPREP, Bruker AXS Inc., Madison, Wisconsin, USA, 2007.
[13] Bruker, SADABS, Bruker AXS Inc., Madison, Wisconsin, USA, 2001.
[14] G.M. Sheldrick, Acta Crystallogr., Sect. A 64 (2008) 112.
[15] K. Brandenburg, DIAMOND Crystal Impact GbR, Bonn, Germany, 1999.
[16] J.Y. Niu, Z.L. Wang, J.P. Wang, Polyhedron 23 (2004) 773.
[17] K. Liu, F.-X. Meng, Y.-G. Chen, Transition Met. Chem. 32 (2007) 343.
[18] J. Sha, J. Peng, J. Chen, H. Liu, A. Tian, P. Zhang, Solid State Sci. 9 (2007) 1012.
[19] M. Fleck, L. Bohaty, Acta Crystallogr., Sect. C 62 (2006) m22.
[20] D.J. Genther, P.J. Squattrito, K. Kirschbaum, E.J. Yearley, A. Pinkerton, Acta Crystallogr., Sect. C 63 (2007) m604.
[21] H. Zhong, H.-L. Xie, C.-J. Luo, Angew. Chem., Int. Ed. Engl. 34 (1995) 1555.
[22] X. Wang, C. Qin, E. Wang, Y. Li, N. Hao, L. Xu, Inorg. Chem. 43 (2004) 1850.
[23] N.E. Brese, M. O'Keeffe, Acta Crystallogr., Sect. B 47 (1991) 192.
[24] I.D. Brown, D. Altermatt, Acta Crystallogr., Sect. B 41 (1985) 244.
[25] H.H. Thorp, Inorg. Chem. 31 (1992) 1585.
[26] K. Nomiya, M. Miwa, R. Kobayash, M. Aiso, Bull. Chem. Soc. Jpn. 54 (1981) 2983.
[27] F. Hajlaoui, H. Naïli, S. Yahyaoui, M.M. Turnbull, T. Mhiri, T. Bataille, Dalton Trans. 40 (2011) 11613.